Frontiers in Bioscience Landmark

Front. Biosci. (Landmark Ed) **2026**; 31(8): 51975
https://doi.org/10.31083/FBL51975

Original Research

Beauvericin Exerts Antitumor Effects on Multiple Myeloma by Disrupting the USP9X-Bcl-2 Interaction to Promote Bcl-2 Degradation

Rui Jin[1,2,†], Runfeng Ni[1,2,†], Ning Ding[1,2], Yuchen Tao[1,2], Shuyang Cai[1,2], Yirong Shi[1,2], Milin Liu[1,2], Yirong Chen[1,2], Letian Yu[1,2], Jiahui Lu[1,2,*]

[1]Institute of Hematology, Shanghai Municipal Hospital of Traditional Chinese Medicine, Shanghai University of Traditional Chinese Medicine, 200071 Shanghai, China
[2]Clinical Hematology Center and Institute of Hematology, Shanghai Municipal Hospital of Traditional Chinese Medicine, Shanghai University of Traditional Chinese Medicine, 200071 Shanghai, China
*Correspondence: lujiahui_sci@126.com (Jiahui Lu)
[†]These authors contributed equally.
Academic Editor: Qingping Dou
Submitted: 17 March 2026 Revised: 26 June 2026 Accepted: 3 July 2026 Published: 18 August 2026

Abstract

Background: Beauvericin is a cyclic hexadepsipeptide derived from *Bombyx batryticatus*. It is known as Jiangcan in traditional Chinese medicine and has diverse pharmacological properties, including antitumor, antiviral, insecticidal, and antibacterial effects. However, its specific mechanisms against multiple myeloma (MM) are not fully understood. The aim of this study was to elucidate the mechanism of beauvericin in MM. **Methods:** This study utilized the mouse Sp2/0 cell line, the human U266 cell line, and a subcutaneous tumor allograft model in C57BL/6J mice. Flow cytometry was employed to evaluate apoptosis, and the Cell Counting Kit-8 (CCK-8) assay was used to measure cellular viability. Network pharmacology was employed for target prediction, followed by molecular docking analyses to confirm drug-target interactions. The protein expression levels of Ubiquitin-Specific Protease 9X (USP9X) and Bcl-2 were assessed by Western blotting following USP9X knockdown. Additionally, co-immunoprecipitation assays were performed to evaluate whether beauvericin modulates the Bcl-2/USP9X interaction and affects Bcl-2 ubiquitination. The antitumor effects of beauvericin were further evaluated through *in vivo* experiments. **Results:** Network pharmacology analysis identified 82 MM-related target genes for beauvericin. These included key targets such as Caspase-3, Bcl-2, Matrix metallopeptidase 9 (MMP9), and Caspase-8, which may contribute to the anti-MM effects of beauvericin. Molecular docking revealed strong affinity and stability between beauvericin and Bcl-2. *In vitro* experiments confirmed that beauvericin inhibits MM cell proliferation, promotes apoptosis, and enhances Bcl-2 ubiquitination and degradation by disrupting the interaction between the deubiquitinating enzyme USP9X and Bcl-2. *In vivo* studies demonstrated that beauvericin treatment suppressed the growth of subcutaneous MM tumors C57BL/6J mice. **Conclusion:** Beauvericin may exert its anti-MM effects by disrupting the USP9X-Bcl-2 interaction, thereby promoting Bcl-2 ubiquitination and degradation, and inducing cell apoptosis in MM cells.

Keywords: multiple myeloma; beauvericin; ubiquitination; apoptosis; network pharmacology; USP9X; Bcl-2

1. Introduction

Multiple myeloma (MM) is a hematologic malignancy characterized by uncontrolled growth of monoclonal plasma cells and excessive secretion of monoclonal immunoglobulins, leading to clinical complications such as anemia, renal impairment, bone destruction, and multi-organ dysfunction. MM accounts for approximately 10% of hematologic malignancies, predominantly affecting individuals aged >40 years. Globally, about 100,000 deaths are attributed to MM each year, with incidence rates ranging between 4.5 and 6 per 100,000 individuals [1,2,3]. The current primary therapeutic regimens utilize a combination of proteasome inhibitors and anti-CD38 monoclonal antibodies. However, achieving a complete cure for MM remains challenging, and there is a pressing need to identify more effective therapeutic strategies.

Beauvericin is a fungal metabolite derived from the traditional Chinese medicine Jiangcan (*Bombyx batryticatus*). It was historically utilized to enhance liver function in clinical settings [4,5]. Beauvericin was shown to be effective against hepatocellular carcinoma by modifying the tumor microenvironment. This was accompanied by diverse biological activities including antiviral, antibacterial, and anti-inflammatory effects [6,7]. Beauvericin also exhibits cytotoxic properties against numerous tumor cell lines [8,9,10]. Wätjen et al. [11] demonstrated that beauvericin specifically triggers apoptosis in hepatocellular carcinoma cells. Nonetheless, the underlying molecular mechanisms of beauvericin against MM have yet to be elucidated, and molecular-level investigations remain scarce.

Network pharmacology is widely employed to systematically identify potential biological targets and predict the molecular mechanisms of drugs, whether individually

or in combination. It highlights the multi-target, multi-pathway, and multi-component characteristics, thereby elucidating comprehensive pharmacological actions [12,13]. Previous studies employing network pharmacology have identified key targets in the treatment of MM, including Tumor Protein p53 (TP53), Nuclear Factor Kappa B Subunit 1 (P50), RELA Proto-Oncogene, NF-κB Subunit (P65), and Glycogen Synthase Kinase 3 Beta (GSK3B). These studies have verified the protein and mRNA expression levels in MM cell lines [14,15].

Bcl-2 family proteins are core molecules in the regulation of apoptosis. Members of this family form a complex regulatory network through various interactions, thereby determining cellular survival [16]. In MM, the abnormal overexpression of Bcl-2 is one of the key mechanisms leading to tumor cell resistance to apoptotic signals. Clinical research indicates that Bcl-2 expression is markedly elevated in plasma cells from MM patients, with higher expression linked to advanced clinical stages, therapeutic resistance, and poorer prognoses [17,18]. At the cellular level, elevated Bcl-2 expression inhibits apoptosis in MM by binding pro-apoptotic molecules such as Bcl-2 associated X protein (BAX) and BCL2 Antagonist/Killer (BAK), thereby blocking mitochondrial permeability transition pore formation, preventing cytochrome c release, and suppressing caspase-dependent apoptotic pathways [19]. Moreover, previous investigations have indicated that depletion of USP9X, a deubiquitination enzyme, reduces Bcl-2 protein abundance, consequently promoting apoptosis in glioblastoma cells [20].

The aim of this research was to investigate the anti-MM efficacy of beauvericin and elucidate the underlying molecular mechanisms through comprehensive methodologies that integrate network pharmacology and molecular docking, as well as *in vitro* and *in vivo* experimental validation. The findings of this study could potentially establish a solid experimental basis for the development of beauvericin as a novel therapeutic agent in the treatment of MM.

2. Methods and Materials

2.1 Identification of Beauvericin-Related Targets in MM

To identify beauvericin-related target genes involved in MM, the PubChem database (https://pubchem.ncbi.nlm.nih.gov/), Comparative Toxicogenomics Database (CTD, https://ctdbase.org/), and TargetNet (http://targetnet.scbdd.com/) were searched using the keyword "beauvericin". Genes associated with MM were retrieved from the GeneCards (https://www.genecards.org/) database, OMIM (http://www.omim.org/) database, and DisGeNET (https://disgenet.com/) databases by entering the keyword "multiple myeloma".

2.2 Identification of Common Targets Between Beauvericin and MM

To investigate interactions between beauvericin and targets associated with MM, target genes identified for beauvericin and MM were analyzed using Venny 2.1.0 (Centro Nacional de Biotecnología, Madrid, Comunidad de Madrid, Spain) (https://bioinfogp.cnb.csic.es/tools/venny/index.html). A Venn diagram was then constructed to visualize overlapping targets.

2.3 Construction of PPI Network

In order to limit the STRING (https://string-db.org/) platform to Homo sapiens, the common targets shared by beauvericin and MM were imported. All other variables were kept at their default values, and a minimum interaction confidence score of 0.4 was imposed. Unrelated nodes were deleted. After that, Cytoscape v3.10.0 (Cytoscape Consortium, Seattle, WA, USA) was used to build and display the resulting protein-protein interaction (PPI) network. Node size and color intensity mirrored the magnitude of the relevant Degree scores, whereas hub genes were screened based on Degree values. The NetworkAnalyzer tool within Cytoscape was used to calculate network topological attributes. After refinement, a regulatory network illustrating "component-target interactions" was constructed.

2.4 Gene Ontology (GO) and Kyoto Encyclopedia of Genes and Genomes (KEGG) Enrichment Analysis

Functional annotation analyses were conducted with the DAVID (https://davidbioinformatics.nih.gov/) bioinformatics database, which encompassed Gene Ontology (GO) enrichment and Kyoto Encyclopedia of Genes and Genomes (KEGG) pathway analysis, among others. Bar plots were used to depict the top 10 enriched phrases that met the threshold of $p < 0.05$. Biological processes (BP) that were considerably enriched were chosen for GO analysis according to p-values. Bubble plots were used to display the top 20 pathways after screening for KEGG pathways that were considerably enriched ($p < 0.05$).

2.5 Verification of Molecular Docking

Molecular docking to evaluate target interactions was performed with AutoDock 4 (Scripps Research Institute, La Jolla, CA, USA) and AutoDock Vina (Scripps Research Institute, La Jolla, CA, USA) software, along with the PyMOL (Schrödinger, Inc., New York, NY, USA) Python sub-program for detailed analysis. Chem3D (PerkinElmer, Inc., Waltham, MA, USA) facilitated the processing of chemical structures. Two-dimensional chemical structures were obtained from the PubChem database, and three-dimensional (3D) protein structures were sourced from the Protein Data Bank (PDB) (https://www.rcsb.org/). Chem3D software converted active ingredient structures to their minimum energy 3D forms. Subsequently, AutoDock 4 was used for dehydration and hydrogenation

preprocessing. Batch molecular docking was conducted using AutoDock Vina and Open Babel, adhering to semi-rigid docking principles. Binding energies below −7.0 kcal/mol served as selection criteria, and the top 20 docking results underwent in-depth analysis with PyMOL. This produced visualizations that highlight molecular binding sites and bond lengths.

2.6 Cell Culture

Human U266 cells (QuiCell-U240) and mouse Sp2/0 cells (QuiCell-S243) were purchased from QuiCell Biotechnology Co., Ltd. (Shanghai, China). STR profiling was used to confirm the origin of cells, and no mycoplasma contamination was detected. The cells were grown in a humidified incubator with 5% CO_2 at 37 °C in RPMI-1640 (Gibco, cat#C11875500BT, Waltham, MA, USA) media supplemented with 10% fetal bovine serum (Gibco, cat#2168090RP, Waltham, MA, USA) and 1% penicillin-streptomycin solution (cat#2585644, Waltham, MA, USA). The final concentration of dimethyl sulfoxide (DMSO) in the culture medium was adjusted to ≤0.1% after preparing a stock solution of 10 mM of beauvericin (MCE, cat# HY-N6739, Monmouth Junction, NJ, USA) in DMSO (Beyotime, cat# ST038, Shanghai, China).

2.7 Lentiviral Construction of USP9X Knockdown Cells

Lentivirus-stable USP9X knockdown (shUSP9X) cell lines for U266 and Sp2/0 were established using specially designed short hairpin RNAs (shRNAs).Target sequences for U266 cells were: shUSP9X-h1: 5′-CCGGTGATGAGAAGTATGAACTGAACTCGAGTTCAGTTCATACTTCTCATCATTTTTG-3′; shUSP9X-h2: 5′-CCGGCCAGTATGTTGATGATATCAACTCGAGTTGATATCATCAACATACTGGTTTTTG-3′; Target sequences for Sp2/0 cells were: shUSP9X-m1: 5′-CCGGGGTTCAAGATCCTGATGATGACTCGAGTCATCATCAGGATCTTGAACCTTTTTG-3′; shUSP9X-m2: 5′-AATTCAAAAAGGTTCTGATCAGGATCTTGAACCTCGAGTCATCATCAGGATCTTGAA-3′.

Lentiviral vectors containing these shRNAs were transfected into HEK-293T cells (STCC10301P) purchased from Servicebio Biotechnology Co., Ltd. (Wuhan, China). Viral particles were then used to infect U266 and Sp2/0 cells. Puromycin was employed to select stable knockdown cells.

2.8 Cell Viability Assay

The CCK-8 assay was used to measure cell proliferation. Briefly, U266 and Sp2/0 cells (1×10^4 cells per well) were plated into 96-well plates. Beauvericin was added to a final concentration of 0, 2.5, 5, 10, and 20 μM, and the cells were cultured for 12, 24, or 48 h at 37 °C with 5% CO_2. Subsequently, 10 μL of CCK-8 reagent (Beyotime, cat#C0037) was added to each well and incubated in darkness for another 2 h. A microplate spectrophotometer (Molecular Devices, San Jose, CA, USA) was then used to measure absorbance values at 450 nm. The percentage of viable cells was determined using the following formula: viability (%) = [(OD_beauvericin − OD_blank)/(OD_control − OD_blank)] × 100%.

The control group consisted of RPMI-1640 medium, serum, antibiotics, cells, and 0.1% DMSO; the blank group was cell-free and contained PBS with 0.1% DMSO. The beauvericin group also comprised cells and beauvericin.

2.9 Flow Cytometry Analysis of Apoptosis

In order to detect apoptosis, U266 and Sp2/0 cells were seeded onto six-well plates (5×10^5 cells per well) and incubated with beauvericin at concentrations of 0, 2.5, 5, and 7.5 μM for 24 h. They were subsequently incubated at 37 °C for 10 min in the dark and then labeled with an Annexin V-FITC/PI apoptosis detection kit (Beyotime, cat#C1062S, Shanghai, China). The rate of apoptosis was measured using flow cytometry, a technique developed by Beckman Coulter in the USA. The gating strategy was as follows: (i) Cells were first gated on a forward scatter (FSC-A) versus side scatter (SSC-A) plot to exclude debris and cell aggregates. (ii) Single cells were gated using FSC-H versus FSC-A to exclude doublets. (iii) The fluorescence intensities of FITC (Annexin V) and PI were compensated using single-stained positive controls (Annexin V-FITC single stain and PI single stain) and an unstained negative control. (iv) Quadrant gates were set based on the untreated control group (0 μM beauvericin), with the lower left quadrant defining the viable cell population. (v) Early apoptotic cells were defined as Annexin V-FITC-positive/PI-negative (Q3), late apoptotic/secondary necrotic cells as Annexin V-FITC-positive/PI-positive (Q2), and primary necrotic cells as Annexin V-FITC-negative/PI-positive (Q1). The percentage of total apoptotic cells was calculated as Q2 + Q3.

2.10 Western Blotting and Co-IP

For the analysis of protein expression, U266 and Sp2/0 cells (5×10^5 per well) were incubated with beauvericin at concentrations of 0, 2.5, 5, 7.5 μM for 24 h. Total protein was extracted on ice using RIPA lysis buffer (cat#BC3710, Solarbio Science & Technology, Beijing, China), and the concentration measured using a BCA protein assay kit (cat#PC0020, Solarbio Science & Technology, Beijing, China). Equal amounts of proteins were separated through 5%–15% SDS-PAGE and transferred onto PVDF membranes (cat#E801-01, Vazyme Biotech Co., Ltd, Nanjing, Jiangsu, China). Membranes were blocked with Rapid Blocking Solution (Servicebio, G2052-500ML) for 1 h at room temperature and incubated overnight at 4 °C with primary antibodies against Bcl-2 (cat#F0125, Selleck Chemicals, Houston, TX, USA), USP9X (cat#F1387, Selleck Chemicals, Houston, TX, USA), and GAPDH (cat#F0003, Selleck Chemicals, Houston, TX, USA) at a dilution ratio of 1:1000. After washing, the membranes were incubated

with secondary antibodies, including anti-rabbit IgG H&L (cat#ab175781, Cambridge, UK) and goat anti-mouse IgG H&L (cat#ab175775, Cambridge, UK), diluted 1:10,000 for 1 h. Protein bands were visualized using an ECL chemiluminescence kit (cat#BL532B, Biosharp Biotechnology, Hefei, Anhui, China) and detected with the Tanon 5200 imaging system.

For co-immunoprecipitation (Co-IP) assays, 1×10^6 cells were lysed in IP buffer and incubated with antibody-conjugated agarose beads. The precipitated complexes were subsequently subjected to Western blot analysis, with IgG serving as the negative control. Relative protein band intensities were quantified using the Tanon 5200 imaging platform.

2.11 Mouse Sp2/0 Model of MM

All animal procedures adhered strictly to ARRIVE guidelines, the UK Animals (Scientific Procedures) Act 1986, the associated guidance, and the National Research Council's animal care guidelines. Ethics approval was granted by the Experimental Animal Ethics Committee of Shanghai Municipal Hospital of Traditional Chinese Medicine, affiliated with Shanghai University of Traditional Chinese Medicine (Approval No.: DW2020014, originally approved in 2020 and extended for this study). Male C57BL/6J mice (8–10 weeks old, 20 ± 2 g) sourced from Beijing Spefo Biotechnology Co., Ltd. were housed under specific pathogen-free conditions at 19–23 °C, 50 ± 20% humidity, with a 12-h light-dark cycle.

The subcutaneous tumor model involved the injection of a 200 µL suspension containing 5×10^6 Sp2/0 cells into the right axillary region of mice. Each of the four experimental groups, consisting of six animals each, was treated with a different dosage of beauvericin as follows: control group (PBS), 3 mg/kg, 6 mg/kg, 9 mg/kg. On days 0, 7, and 14, mice received intraperitoneal injections of either beauvericin or PBS. Animal body weights were recorded weekly. On day 21, mice were deeply anesthetized by intraperitoneal injection of sodium pentobarbital (50 mg/mL solution, 0.1 mL per 10 g body weight). Depth of anesthesia was confirmed by loss of corneal reflex and absence of response to toe pinch. Euthanasia was then completed by cervical dislocation. Death was confirmed by cessation of breathing, absence of heartbeat, and lack of corneal reflex. Histopathological analysis and TUNEL staining involved the removal, weighing, and photographing of tumor samples followed by fixation in 4% paraformaldehyde. Blood samples were also taken in order to assess serum biochemical parameters such as ALT, AST, BUN, and Cr. Major organs, including the kidneys, lungs, liver, spleen, and heart, were extracted for H&E staining.

2.12 Statistical Analysis

SPSS version 26.0 (IBM Corp., Armonk, NY, USA) was used for statistical analyses, while GraphPad Prism 10.0 (GraphPad Software, San Diego, CA, USA) was applied for graphical visualization. All experimental data were expressed as the mean ± standard deviation (SD). Statistical analyses were performed using one-way analysis of variance (ANOVA), followed by Student's *t*-test for pairwise comparisons. Differences with a *p*-value of <0.05 were considered statistically significant.

3. Results

3.1 Identification of Potential Target Genes for MM and Beauvericin

A total of 5005 MM target genes were retrieved from the GeneCards database, OMIM database, and DisGeNET databases. Moreover, 169 potential target genes of beauvericin were identified by searching the PubChem, CTD, and TargetNet databases. Using $p < 0.05$ as the reference value, we identified 82 common target genes that intersect with the obtained MM target genes. They are plotted in a Venn diagram (Fig. 1A) and are considered to present potential therapeutic targets.

3.2 Construction of PPI Network and Functional Analysis of Key Genes

The PPI network was obtained by searching the STRING database for the 82 common target genes (Fig. 1B). This network illustrates the complex interactions among targets, where nodes represent targets and edges denote interactions between different proteins. The PPI network comprised 79 nodes and 357 edges. The top 20 targets ranked by degree are listed in Table 1.

Table 1. The top 20 targets ranked by degree.

No.	Target	Degree
1	ACTB	43
2	CASP3	40
3	BCL2	34
4	MMP9	27
5	CASP8	21
6	MDM2	20
7	CXCL8	19
8	AR	19
9	CASP9	18
10	HNF4	16
11	BCL2A1	16
12	BIRC3	15
13	HDAC2	15
14	CEBPB	14
15	PTPRC	14
16	BIRC2	14
17	ABCB1	13
18	CYP3A4	13
19	HDAC4	13
20	DNMT1	13

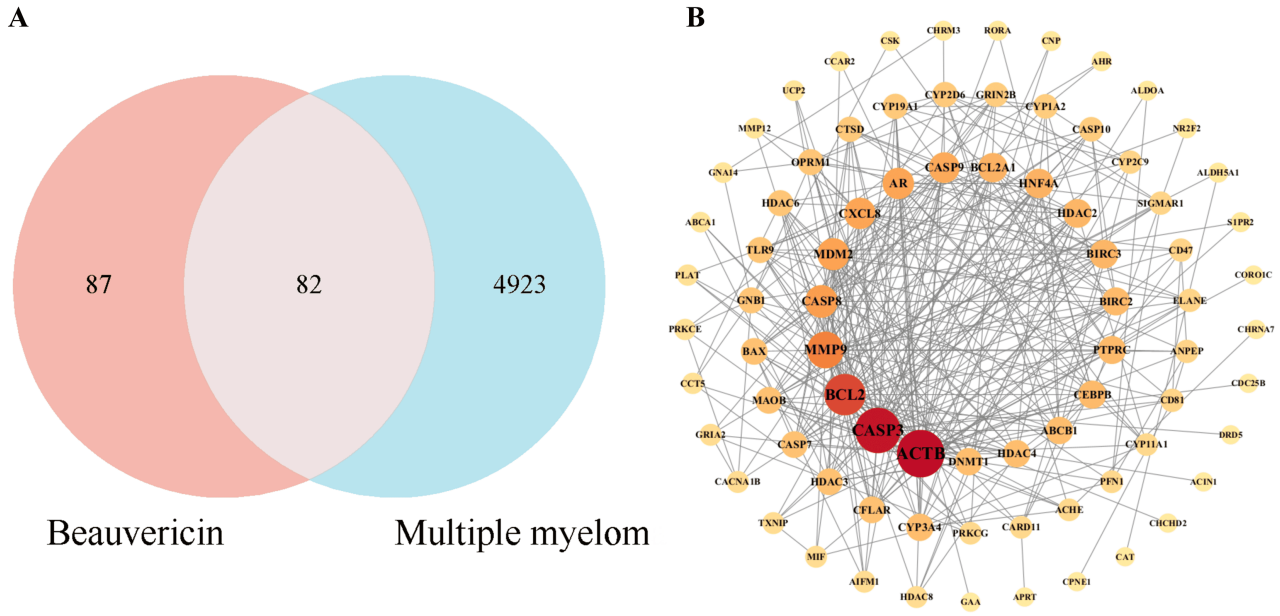

Fig. 1. Identification of potential targets for beauvericin and MM, along with the protein-protein interactions (PPI) network. (A) Venn diagram of targets identified for beauvericin and MM. (B) Construction of a PPI network incorporating all proteins (or genes). Nodes represent targets, and connections denote interactions between different target proteins.

Table 2. Molecular docking scores.

Target	Docking score (kcal/mol)	Amino acid residues
Caspase-3	–6.5	SER-381, ARG-341, THR-177, PHE-381
Bcl-2	–8.7	GLU-95, LEU-96, ARG-105, TYR-67
MMP9	–7.3	ARG-143, GLU-427
Caspase-8	–6.8	GLN-32, LEU-27, ARG-102, GLU-147

3.3 GO Analysis and KEGG Pathway Enrichment Analysis

The DAVID database was utilized to perform enrichment analysis, identifying relevant BP, Cellular Components (CC), and Molecular Functions (MF). This analysis yielded 352 GO terms, comprising 224 in Biological Process, 45 in Cellular Component, and 83 in Molecular Function categories (Fig. 2A). Furthermore, KEGG pathway analysis revealed 75 enriched signaling pathways. The top 20 pathways, ranked by their respective *p*-values, are illustrated through a bubble chart for clear visualization in Fig. 2B. The results suggest that beauvericin may significantly influence apoptosis in MM. By integrating this information with the PPI network data (Fig. 1B), we postulate that beauvericin may act on MM by targeting apoptosis.

3.4 Molecular Docking Between Beauvericin and the Targets Related to Apoptosis

Molecular docking simulations were conducted in order to validate the interaction of beauvericin with identified critical targets (Fig. 3). Results indicated that beauvericin demonstrated higher binding affinity for Bcl-2 compared with other assessed targets (Caspase-3, MMP9, Caspase-8). Docking scores and interacting amino acid residues are detailed in Table 2. In subsequent experiments, we therefore focused on Bcl-2 for further investigation.

3.5 Beauvericin Inhibits MM Cell Proliferation and Induces Apoptosis in a Dose- and Time-Dependent Manner

Cell viability assays using the CCK-8 method revealed that beauvericin markedly suppressed proliferation in U266 and Sp2/0 cells in both dose- and time-dependent patterns (Fig. 4A). IC_{50} values for U266 cells were calculated at 8.11 ± 0.10 μM (12 h), 7.90 ± 0.17 μM (24 h), and 3.27 ± 0.19 μM (48 h). The IC50 values for Sp2/0 cells were calculated as 8.24 ± 0.10 μM (12 h), 7.84 ± 0.10 μM (24 h), and 5.23 ± 0.13 μM (48 h) for Sp2/0 cells. To confirm if apoptosis contributed to reduced viability, cells were exposed to beauvericin (0, 2.5, 5, and 7.5 μM) for 24 h, stained using Annexin V-FITC/PI, and analyzed by flow cytometry. Compared to untreated controls, the apoptotic rate increased progressively with escalating concentrations of beauvericin (Fig. 4B). Since the molecular docking analysis indicated the highest affinity was between beauvericin and Bcl-2, further investigations focused on the role of Bcl-2. Western blot analysis confirmed that beauvericin significantly re-

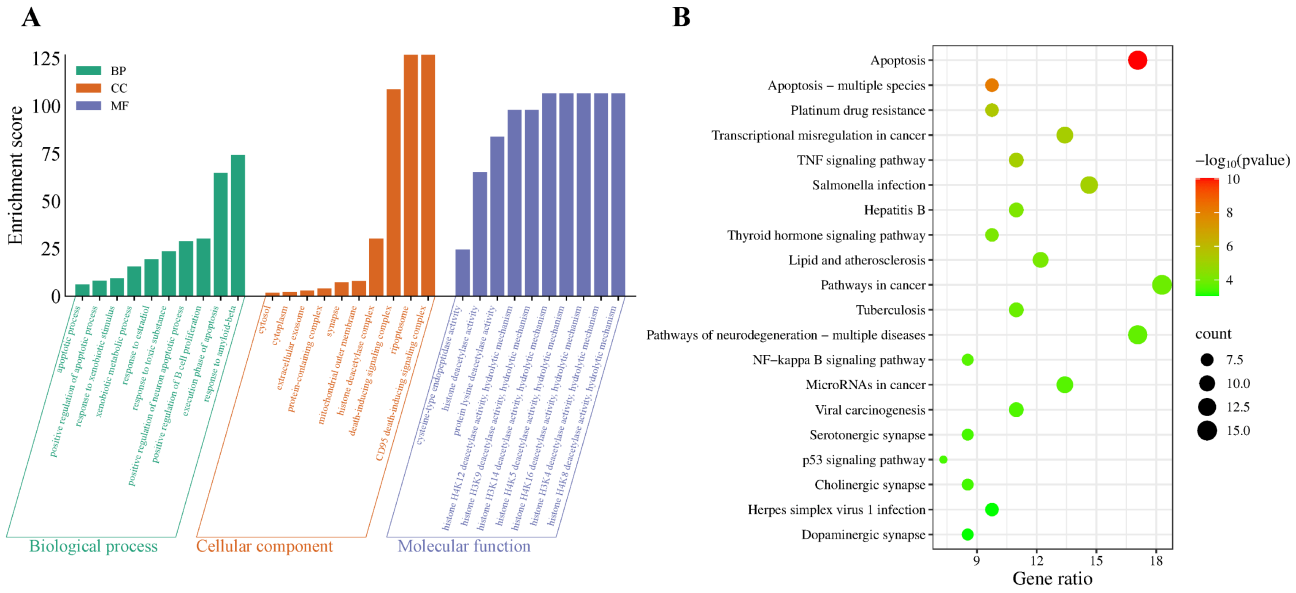

Fig. 2. Gene Ontology (GO) and Kyoto Encyclopedia of Genes and Genomes (KEGG) enrichment analyses of target genes affected by beauvericin. (A) Distribution of 82 target genes across the Biological Processes (BP), Cellular Components (CC), and Molecular Functions (MF) categories. (B) KEGG enrichment analysis showing enriched pathways. The x-axis indicates the ratio of the target proteins to background proteins, while the y-axis represents the pathways. Bar color intensity corresponds to the $-\log_{10}(p)$ values.

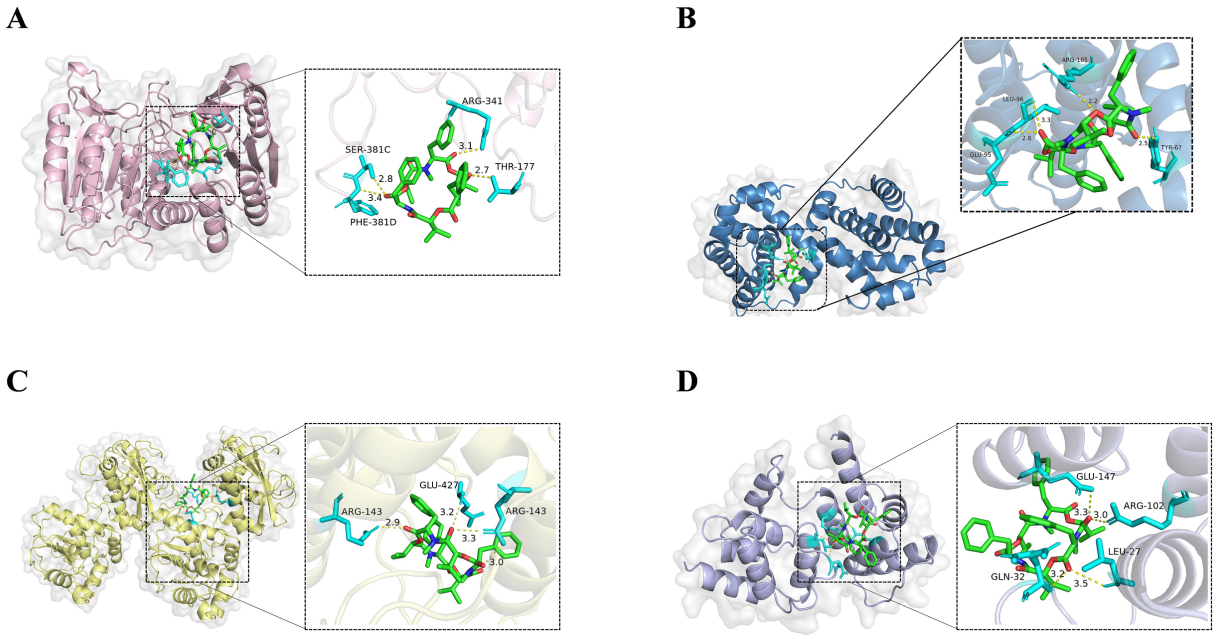

Fig. 3. Beauvericin binds to the apoptosis-related target. (A) Caspase-3. (B) Bcl-2. (C) MMP9. (D) Caspase-8.

duced Bcl-2 protein expression in a dose-dependent manner in both cell lines (Fig. 4C).

3.6 Beauvericin Promotes Bcl-2 Degradation by Disrupting the USP9X-Bcl-2 Interaction

Previous studies have reported that the deubiquitinating enzyme USP9X can specifically remove ubiquitin chains from the anti-apoptotic protein Bcl-2, thereby inhibiting its ubiquitin-mediated degradation and maintaining its stability [21,22]. We first treated both cell types with MG132 (10 μM) for 4 h, followed by treatment with beauvericin (10 μM) for 24 h. Co-immunoprecipitation (Co-IP) experiments revealed that beauvericin modulates the endogenous interaction between USP9X and Bcl-2 in multi-

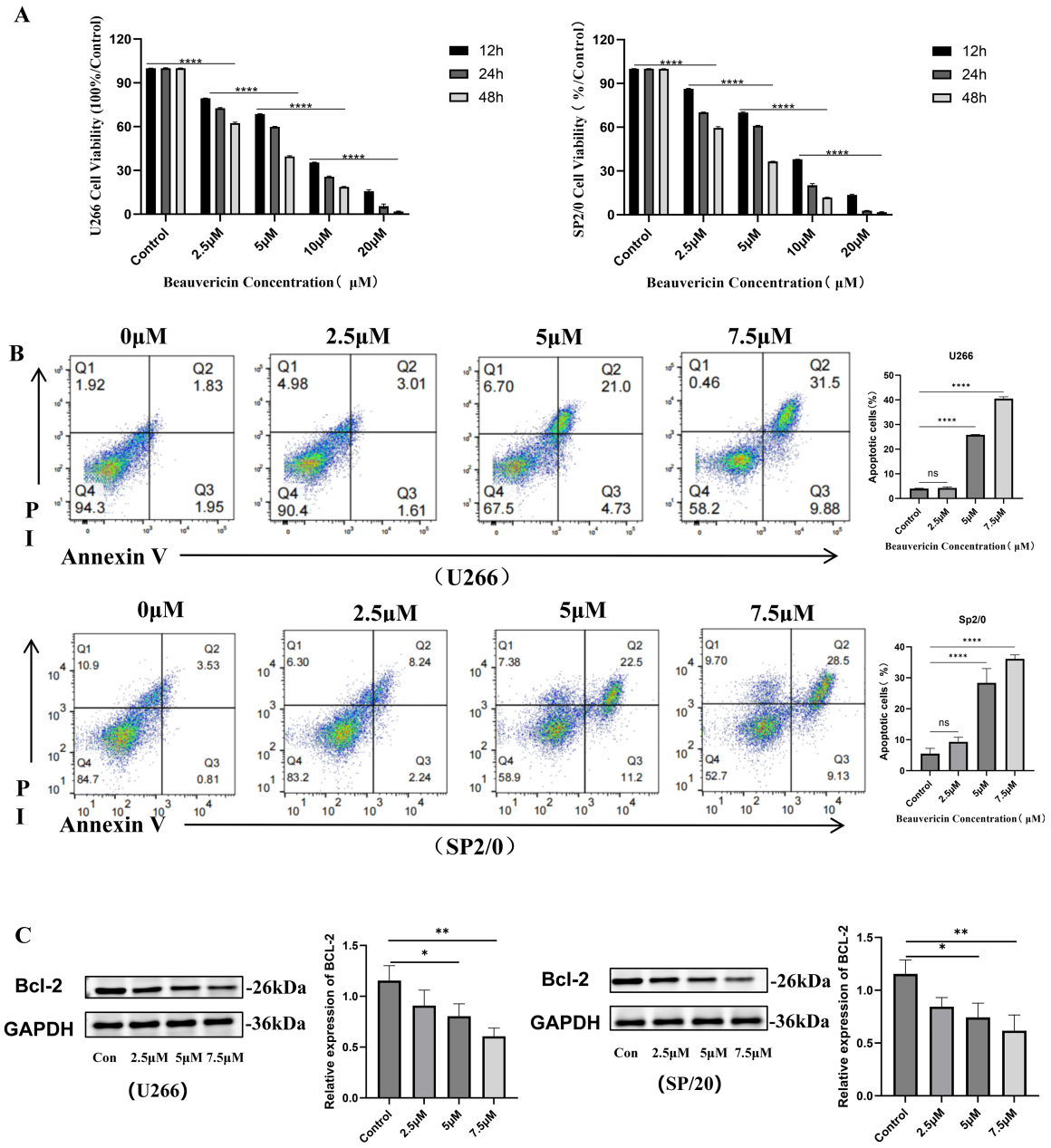

Fig. 4. Beauvericin induces apoptosis in MM cells. (A) Dose- and time-dependent impact of beauvericin on MM cell viability. ****$p <$ 0.0001 compared to untreated controls (0 μM beauvericin). (B) Quantification of apoptosis via flow cytometry. The percentage of apoptotic cells was calculated as the sum of early apoptotic cells (Annexin V-positive/PI-negative, Q3 quadrant) and late apoptotic/necrotic cells (Annexin V-positive/PI-positive, Q2 quadrant). The bar graph presents the total apoptotic cell percentage (Q2+Q3) for each treatment condition. ****$p < 0.0001$, compared with control group (beauvericin = 0 μM). ns, not significant. (C) U266 and Sp2/0 cells were treated with beauvericin (0–7.5 μM) for 24 h, and the level of Bcl-2 expression was then assessed by Western blot analysis. *$p < 0.05$; **$p < 0.01$, compared with control group (beauvericin = 0 μM).

ple myeloma cells, as shown in Fig. 5A. Next, we knocked down USP9X in both MM cell lines, the shUSP9X-h2 (U266) and shUSP9X-m1 (Sp2/0) constructs exhibited the best knockdown efficiency (Fig. 5B) and were selected for subsequent experiments. To study the deubiquitination effect of USP9X on Bcl-2 in MM cells, we subsequently performed Co-IP experiments. Compared to the control group, Bcl-2 ubiquitination levels were found to be significantly higher after USP9X was knocked down (Fig. 5C).

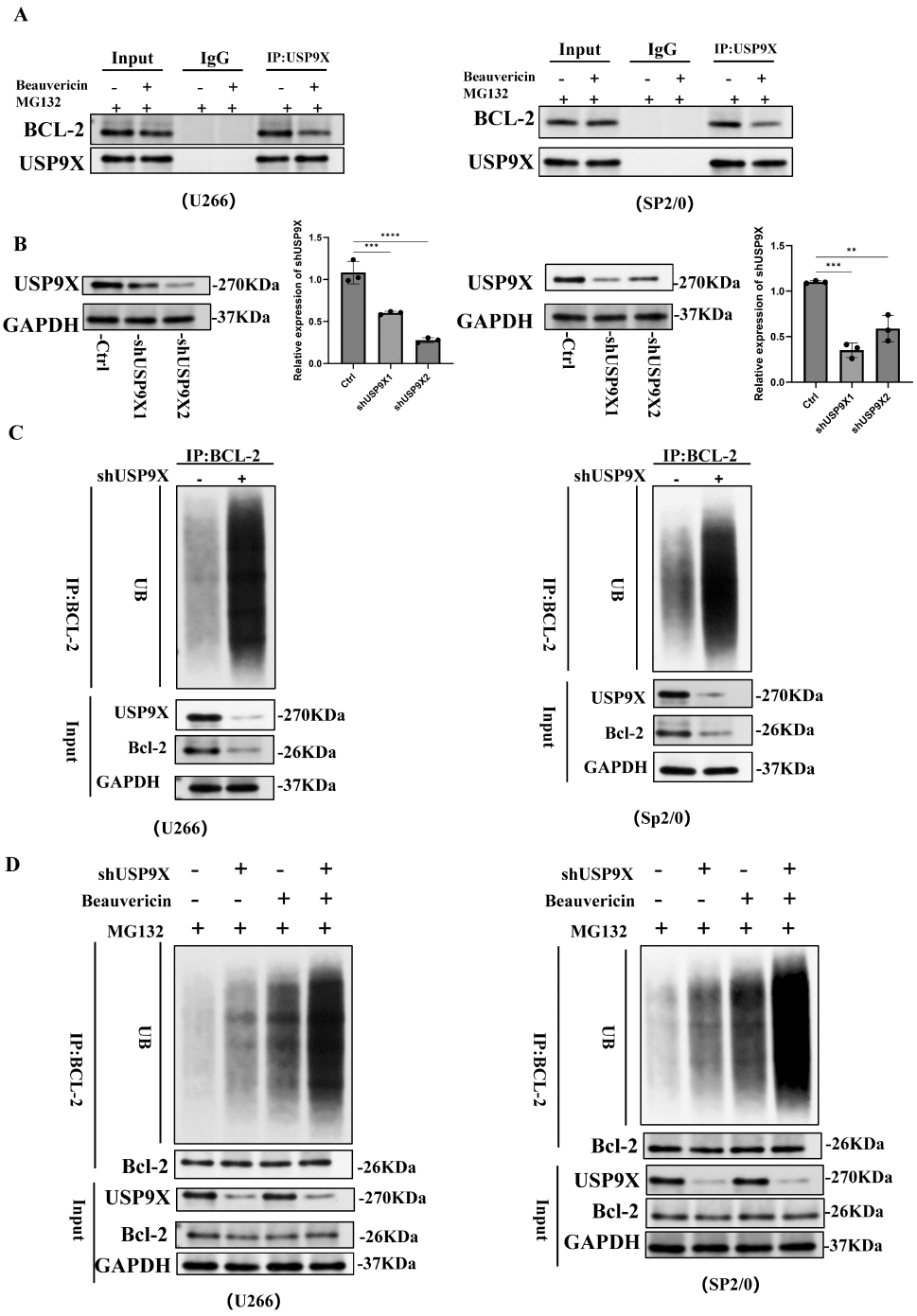

Fig. 5. Beauvericin interferes with USP9X-mediated ubiquitination and promotes Bcl-2 ubiquitination-mediated degradation. (A) Beauvericin affects the endogenous interaction between USP9X and Bcl-2 in MM cells. (B) Knockdown efficiency of USP9X in MM cells, $^{**}p < 0.01$, $^{***}p < 0.001$; $^{****}p < 0.0001$, compared with the control group. (C) USP9X knockdown enhances Bcl-2 ubiquitination. (D) Beauvericin promotes Bcl-2 ubiquitination-mediated degradation by inhibiting USP9X-Bcl-2 binding activity.

Finally, to investigate whether beauvericin promotes Bcl-2 ubiquitination-mediated degradation, U266 and Sp2/0 cells were pretreated with MG132 (10 μM) for 4 h and subsequently treated with beauvericin (10 μM) for 24 h. Beauvericin treatment significantly increased Bcl-2 ubiquitination levels compared to the control group (Fig. 5D). Furthermore, when USP9X was knocked down, beauvericin treatment further enhanced this ubiquitination process. Collectively, these results indicate that beauvericin promotes Bcl-2 ubiquitination and degradation in MM cells by disrupting the USP9X-Bcl-2 interaction in MM cells, ultimately inducing MM cell apoptosis.

3.7 Beauvericin Suppresses Tumor Growth In Vivo

We next established a Sp2/0 cell allograft tumor model in C57BL/6J mice to evaluate the antitumor efficacy of beauvericin. After successful modeling, Sp2/0 mice received intraperitoneal injections of different doses of beauvericin on days 0, 7, and 14, and we euthanized on day 21. Compared with the control group, beauvericin at doses of 3, 6, and 9 mg/kg significantly inhibited tumor growth (Fig. 6A), which manifested primarily manifested as reduced tumor volume. No significant differences in body weight were observed between groups during drug administration (Fig. 6B). Statistical analysis indicated that beauvericin significantly suppressed tumor growth in the Sp2/0 tumor-bearing mouse model (Fig. 6C). TUNEL staining revealed that beauvericin significantly promoted tumor cell apoptosis (Fig. 6D,E). Finally, serum biochemistry and histopathological examination of major organs confirmed the absence of treatment-related toxicity in beauvericin-treated mice. (**Supplementary Fig. 1** and **Supplementary Table 1**). Collectively, these results demonstrate that beauvericin promotes apoptosis in Sp2/0 cells while significantly inhibiting tumor growth in Sp2/0 tumor-bearing mice.

4. Discussion

Numerous studies have indicated that beauvericin possesses potent antitumor effects against a variety of malignancies, including hepatocellular carcinoma [4], osteosarcoma [23], and breast cancer [24]. In hematological research, beauvericin was shown to induce apoptosis in HL-60 leukemia cells, highlighting its therapeutic potential for the management of leukemia [25]. Building upon previous evidence regarding the antitumor properties of beauvericin, the present study utilized network pharmacology coupled with molecular docking methods to explore its efficacy against MM. Our findings confirmed the significant inhibitory effects of beauvericin on MM cell proliferation, induction of apoptosis, and suppression of tumor growth in animal models, without observable toxicity in treated mice. We also further elucidated the underlying its anti-MM mechanisms of beauvericin.

Network pharmacology offers insights into drug-disease interactions through systems biology and network equilibrium concepts. Notably, the current research represents the first application of a network pharmacology framework to evaluate the therapeutic role of beauvericin in MM, adding substantial evidence in support of its potential involvement in MM treatment.

Analysis of the PPI network highlighted the complex interactions among beauvericin-associated anti-MM targets rather than isolated molecular effects. This study identified critical targets through which beauvericin may exert therapeutic efficacy, including Caspase-3, Bcl-2, MMP9, and Caspase-8. Caspase-3 is an essential effector enzyme within apoptosis pathways and mediates the cleavage of key substrates, culminating in DNA fragmentation, cytoskeletal disintegration, and cell apoptosis in MM [26]. Bcl-2 is a pivotal anti-apoptotic regulator within the mitochondrial apoptotic cascade. Its expression is frequently elevated in MM cells, contributing to resistance against chemotherapeutic and targeted treatments [27]. MMP9 serves as a prominent biomarker associated with MM-induced bone disease. It facilitates bone matrix degradation and tumor progression, and is detectable in approximately 65% of bone marrow biopsies from MM patients [28]. Caspase-8 functions as an important initiator of apoptosis via TNF-related apoptosis-inducing ligand (TRAIL) signaling pathways in MM [29].

To delve deeper into the mechanisms underlying the action of beauvericin against MM, we conducted GO functional annotation and KEGG pathway enrichment analyses. This revealed significant associations of critical target genes with BP, CC, and MF. KEGG analysis highlighted several pivotal pathways linked to MM pathogenesis, including apoptosis regulation, platinum-based drug resistance, TNF signaling, and general cancer pathways. Dysregulation of apoptosis pathways has been established as a fundamental mechanism underlying MM pathogenesis and therapeutic resistance. Additionally, the TNF signaling pathway is critically involved in inflammation, immune regulation, and cancer development and progression [30].

In vivo studies into the antitumor efficacy of beauvericin demonstrated dose-dependent suppression of subcutaneous Sp2/0 tumor growth. Additionally, serum biochemical analyses and histopathological examinations of major organs in treated mice revealed no evident treatment-associated toxicity (**Supplementary Fig. 1** and **Supplementary Table 1**). Beyond tumor inhibition, we explored the apoptotic mechanisms induced by beauvericin in MM cell proliferation. Dose-dependent apoptosis induction by beauvericin in MM cells was also confirmed by flow cytometry analyses. Results of Western blot analysis further verified that beauvericin reduces the expression of anti-apoptotic Bcl-2 protein in a dose-dependent manner.

A critical question arising from our findings is how beauvericin achieves selective disruption of the USP9X-Bcl-2 PPI without globally perturbing USP9X expression or catalytic activity. Based on the convergence of our existing experimental data, we propose a multi-layered mechanistic framework that integrates structural, biochemical, and functional perspectives.

Our molecular docking analysis revealed that beauvericin binds to Bcl-2 with high affinity (docking score: −8.7 kcal/mol), engaging residues within and adjacent to the BH3-binding groove (GLU-95, LEU-96, ARG-105, TYR-67). The USP9X-Bcl-2 interaction has been reported to involve the C-terminal tail of Bcl-2 and adjacent hydrophobic residues that partially overlap with this region. We hypothesize that beauvericin acts as an interfacial inhibitor by occupying a Bcl-2 surface that sterically or al-

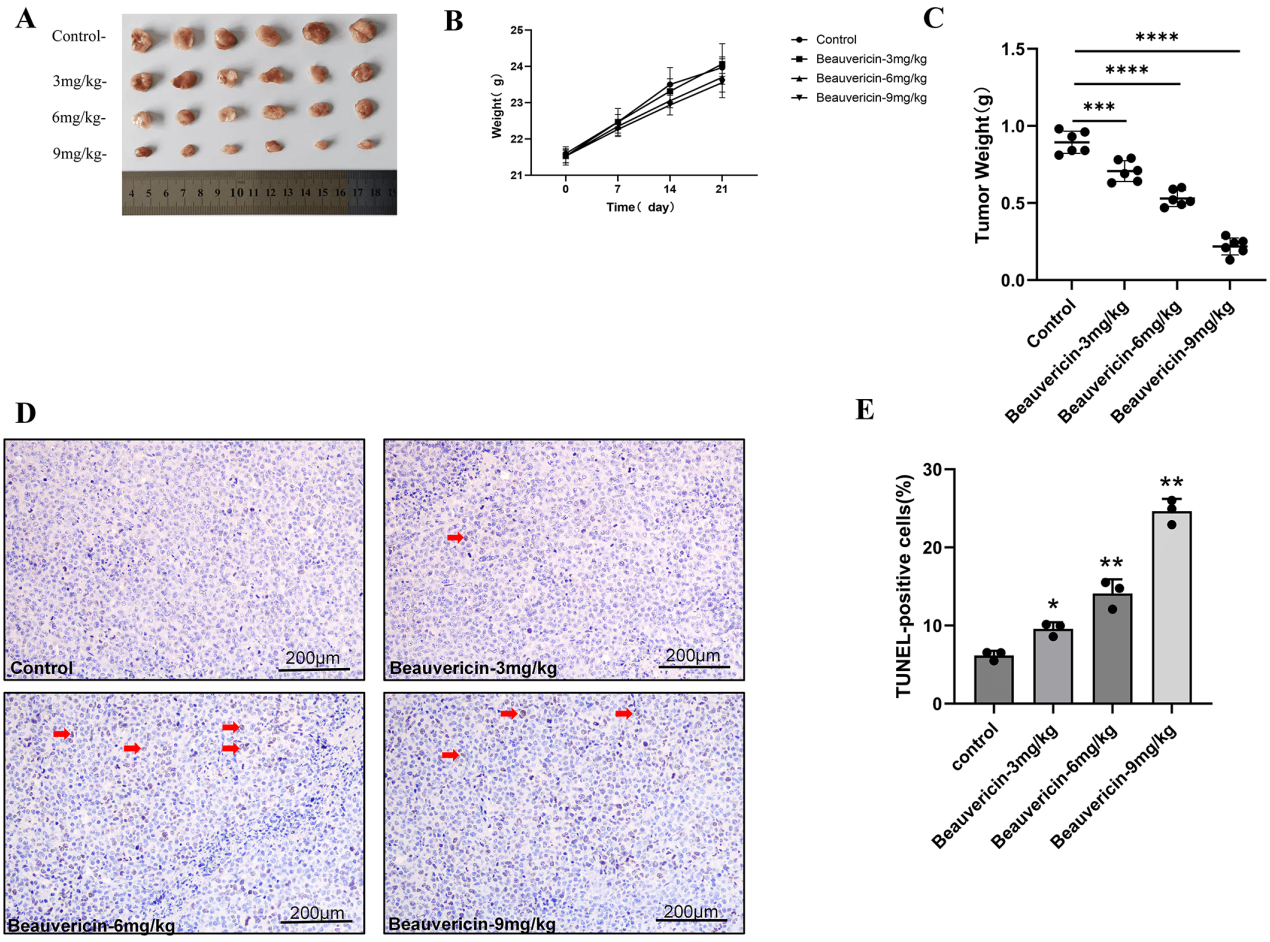

Fig. 6. Beauvericin suppresses tumor growth *in vivo*. (A) Photographs of tumors obtained from tumor-bearing mice following beauvericin treatment. (B) Weekly measurement of mouse body weight. (C) Tumor weight in different treatment groups. n = 6 mice per group. ***$p < 0.001$; ****$p < 0.0001$ compared with control group. (D,E) Detection of apoptotic cells (red arrows in D) by TUNEL assay (*$p < 0.05$, **$p < 0.01$) (magnification: 200×, scale bar = 200μm). n = 6 mice per group.

losterically interferes with USP9X recruitment. This hypothesis is directly supported by our bidirectional Co-IP data (Fig. 5A). Furthermore, Bcl-2 ubiquitination levels increase following treatment with beauvericin or USP9X knockdown (Fig. 5B and Fig. 5C). The absence of protein level reduction rules out transcriptional or translational suppression as the mechanism, favoring a direct physical interference with the PPI interface. The functional consequences of this disruption are evidenced by our ubiquitination cascade. In the absence of beauvericin, USP9X stabilizes Bcl-2 by removing ubiquitin chains; upon beauvericin treatment, the physical separation of USP9X from Bcl-2 (Fig. 5A) permits unrestricted ubiquitination of Bcl-2, as confirmed by the increased ubiquitin signal in our Co-IP assays (Fig. 5D). The MG132 rescue experiment (Fig. 5D) further confirms that the observed Bcl-2 degradation is proteasome-dependent, consistent with the loss of USP9X-mediated deubiquitinase protection. This causal chain—PPI disruption → loss of deubiquitination → ubiquitin accumulation → proteasomal degradation—is fully supported by our existing data without invoking off-target effects on the proteasome itself. This substrate-directed mechanism is pharmacologically advantageous, as global USP9X inhibition would predictably disrupt multiple signaling pathways and induce broad cytotoxicity. The proposed mechanism bears mechanistic analogy to venetoclax, which binds the BH3 groove of Bcl-2 to displace pro-apoptotic BH3-only proteins. However, beauvericin differs fundamentally in its downstream consequence: whereas venetoclax neutralizes Bcl-2's anti-apoptotic function by releasing BAX/BAK, beauvericin promotes Bcl-2 degradation by severing its protective deubiquitinase interaction. This positions beauvericin as a prototype for a distinct class of PPI disruptors that selectively target deubiquitinase-substrate interfaces to induce targeted protein degradation, rather than merely inhibiting protein function.

This study has several limitations. The in vitro experiments were conducted using only two MM cell lines

human U266 and murine Sp2/0. Although these represent distinct MM subtypes, their restricted cellular diversity may limit the generalizability of our findings across the broad molecular heterogeneity of human MM. To confirm translational relevance future investigations should validate the anti-MM effects of beauvericin in additional human MM cell lines (e.g., RPMI-8226, MM.1S, NCI-H929) and, critically, in primary CD138+ plasma cells isolated from MM patients to confirm translational relevance. Secondly, the in vivo efficacy was evaluated exclusively in a subcutaneous Sp2/0 allograft model in immunocompetent C57BL/6J mice. While this model demonstrates the antitumor activity of beauvericin in an immunointact setting, it does not recapitulate the human bone marrow microenvironment, including osteoclast–osteoblast interactions, hypoxic niches, and stromal cell-mediated drug resistance that are pathognomonic of human MM. This study also utilized the allogeneic Sp2/0-C57BL/6J tumor model. Although the high tumor formation rate and sustained tumor growth indicate that this model is suitable for evaluating the antitumor activity of beauvericin, it may not be appropriate for assessing immunotherapeutic interventions, as allogeneic immune responses may interfere with treatment efficacy. It is recommended that future studies be conducted in genotypically matched models (such as the Sp2/0 model in BALB/c mice) for validation, particularly when investigating immunomodulatory mechanisms. Future validation in syngeneic models (e.g., Sp2/0 in BALB/c mice) is recommended, particularly if immunomodulatory mechanisms are to be investigated.

In conclusion, the present findings underscore the notable potential of beauvericin as an antitumor agent, demonstrating pronounced efficacy both in cell-based experiments and *in vivo* subcutaneous allograftmodels. Nonetheless, further research remains necessary to clarify its detailed molecular mechanisms of action. Considering its translational potential, beauvericin may serve as a promising adjunct therapy alongside proteasome inhibitors, further enhancing their collective suppression of the ubiquitin-proteasome signaling pathway. Rigorous clinical investigations are needed to systematically assess the clinical effectiveness and safety profiles associated with therapeutic combinations involving beauvericin.

5. Conclusion

In this comprehensive study, the mechanisms and core targets through which beauvericin exerts its effects against MM were clarified using network pharmacology, molecular docking, and *in vitro* as well as *in vivo* experimental validations. We confirmed Bcl-2 as a critical target for beauvericin, elucidating its antitumor activity via disruption of the USP9X-Bcl-2 interaction, inhibition of USP9X-mediated Bcl-2 deubiquitination, and subsequent proteasomal degradation leading to MM cell apoptosis. These mechanisms effectively induce apoptosis and suppress tumor growth in both cellular and animal models. The insights gained from this investigation lay a foundation for further exploration of the therapeutic mechanisms and clinical potential of beauvericin. This should address current treatment limitations in MM and significantly contribute to the translation of laboratory findings into clinical practice.

Availability of Data and Materials

All source data for this work (or generated in this study) are available upon reasonable request.

Author Contributions

.RJ: Methodology, Investigation. RFN: Methodology, Investigation. ND: Methodology, Investigation. YCT: Methodology, Investigation. RJ and SYC: Investigation, Writing - original draft. YRS: Writing - original draft, Data curation. MLL and YRC: Writing - review & editing, Conceptualization. LTY: Writing - original draft, Data curation. JHL: Writing - review & editing, Conceptualization. All authors contributed to critical revision of the manuscript for important intellectual content. All authors reviewed and approved the final manuscript. All authors have participated sufficiently in the work and agreed to be accountable for all aspects of the work.

Ethics Approval and Consent to Participate

Animal ethics was approved by the Experimental Animal Ethics Committee of Shanghai Municipal Hospital of Traditional Chinese Medicine, affiliated with Shanghai University of Traditional Chinese Medicine (Approval No.: DW2020014). All experimental protocols were performed in accordance with the Guide for the Care and Use of Laboratory Animals (National Institutes of Health, USA) and the ARRIVE guidelines.

Acknowledgment

We thank all individuals who assisted in the preparation of this manuscript, and we gratefully acknowledge the constructive comments and suggestions from peer reviewers.

Funding

This work was supported by grants from the National Natural Science Foundation of China (Grant#82405217).

Conflicts of Interest

The authors declare no conflicts of interest.

Supplementary Material

Supplementary material associated with this article can be found, in the online version, at https://doi.org/10.31083/FBL51975.

References

[1] Kumar SK, Rajkumar V, Kyle RA, van Duin M, Sonneveld P, Mateos MV, et al. Multiple myeloma. Nature Reviews. Disease Primers. 2017; 3: 17046. https://doi.org/10.1038/nrdp.2017.46

[2] van de Donk NWCJ, Pawlyn C, Yong KL. Multiple myeloma. Lancet (London, England). 2021; 397: 410–427. https://doi.org/10.1016/S0140-6736(21)00135-5

[3] Diaz-delCastillo M, Chantry AD, Lawson MA, Heegaard AM. Multiple myeloma-A painful disease of the bone marrow. Seminars in Cell & Developmental Biology. 2021; 112: 49–58. https://doi.org/10.1016/j.semcdb.2020.10.006

[4] Wang G, Qiao Y, Zhao Y, Song Y, Li M, Jin M, et al. Beauvericin exerts an anti-tumor effect on hepatocellular carcinoma by inducing PI3K/AKT-mediated apoptosis. Archives of Biochemistry and Biophysics. 2023; 745: 109720. https://doi.org/10.1016/j.abb.2023.109720

[5] Kyungjin L, Bumjung K, Youngmin B, Hyejin J, Meixiang S, Minwoo K, et al. Review on the characteristics of liver-pacifying medicinal in relation to the treatment of stroke: from scientific evidence to traditional medical theory. Journal of Traditional Chinese Medicine. 2018; 38: 139–150.

[6] Lim HN, Jang JP, Shin HJ, Jang JH, Ahn JS, Jung HJ. Cytotoxic Activities and Molecular Mechanisms of the Beauvericin and Beauvericin G_1 Microbial Products against Melanoma Cells. Molecules (Basel, Switzerland). 2020; 25: 1974. https://doi.org/10.3390/molecules25081974

[7] Hu M, Yu Z, Wang J, Fan W, Liu Y, Li J, et al. Traditional Uses, Origins, Chemistry and Pharmacology of Bombyx batryticatus: A Review. Molecules (Basel, Switzerland). 2017; 22: 1779. https://doi.org/10.3390/molecules22101779

[8] Heilos D, Rodríguez-Carrasco Y, Englinger B, Timelthaler G, van Schoonhoven S, Sulyok M, et al. The Natural Fungal Metabolite Beauvericin Exerts Anticancer Activity In Vivo: A Pre-Clinical Pilot Study. Toxins. 2017; 9: 258. https://doi.org/10.3390/toxins9090258

[9] Lin HI, Lee YJ, Chen BF, Tsai MC, Lu JL, Chou CJ, et al. Involvement of Bcl-2 family, cytochrome c and caspase 3 in induction of apoptosis by beauvericin in human non-small cell lung cancer cells. Cancer Letters. 2005; 230: 248–259. https://doi.org/10.1016/j.canlet.2004.12.044

[10] Yahagi H, Yahagi T, Furukawa M, Matsuzaki K. Antiproliferative and Antimigration Activities of Beauvericin Isolated from *Isaria* sp. on Pancreatic Cancer Cells. Molecules (Basel, Switzerland). 2020; 25: 4586. https://doi.org/10.3390/molecules25194586

[11] Wätjen W, Debbab A, Hohlfeld A, Chovolou Y, Proksch P. The mycotoxin beauvericin induces apoptotic cell death in H4IIE hepatoma cells accompanied by an inhibition of NF-κB-activity and modulation of MAP-kinases. Toxicology Letters. 2014; 231: 9–16. https://doi.org/10.1016/j.toxlet.2014.08.021

[12] Hua Y, Tan X, Zhang J, Xu N, Chen R, Zhou S, et al. Deciphering the pharmacological mechanism of Radix astragali for allergic rhinitis through network pharmacology and experimental validation. Scientific Reports. 2024; 14: 29873. https://doi.org/10.1038/s41598-024-80101-1

[13] Bakhsh HT, Abu-Baih DH, Abu-Baih RH, Saber EA, Altemani FH, Algehainy NA, et al. Unveiling Lobophytum sp. the neuroprotective potential of Parkinson's disease through multifaceted mechanisms, supported by metabolomic analysis and network pharmacology. Scientific Reports. 2024; 14: 21810. https://doi.org/10.1038/s41598-024-66781-9

[14] Wang Y, Zhang A, Chen Y, Qi D, Peng C, Liang Z, et al. Mechanism of Brucea javanica against multiple myeloma via TNF-NF-κB signaling. Scientific Reports. 2025; 15: 24311. https://doi.org/10.1038/s41598-025-10271-z

[15] Zeng J, Luo Q, Wang X, Xie W, Dong S, Fu H. Network pharmacology- and molecular docking-based investigation of the therapeutic potential and mechanism of daucosterol against multiple myeloma. Translational Cancer Research. 2023; 12: 1006–1020. https://doi.org/10.21037/tcr-23-456

[16] Czabotar PE, Lessene G, Strasser A, Adams JM. Control of apoptosis by the BCL-2 protein family: implications for physiology and therapy. Nature Reviews. Molecular Cell Biology. 2014; 15: 49–63. https://doi.org/10.1038/nrm3722

[17] Touzeau C, Maciag P, Amiot M, Moreau P. Targeting Bcl-2 for the treatment of multiple myeloma. Leukemia. 2018; 32: 1899–1907. https://doi.org/10.1038/s41375-018-0223-9

[18] Lernoux M, Schnekenburger M, Dicato M, Diederich M. Susceptibility of multiple myeloma to B-cell lymphoma 2 family inhibitors. Biochemical Pharmacology. 2021; 188: 114526. https://doi.org/10.1016/j.bcp.2021.114526

[19] Youle RJ, Strasser A. The BCL-2 protein family: opposing activities that mediate cell death. Nature Reviews. Molecular Cell Biology. 2008; 9: 47–59. https://doi.org/10.1038/nrm2308

[20] Yamaguchi R, Lartigue L, Perkins G. Targeting Mcl-1 and other Bcl-2 family member proteins in cancer therapy. Pharmacology & Therapeutics. 2019; 195: 13–20. https://doi.org/10.1016/j.pharmthera.2018.10.009

[21] Vaxman I, Sidiqi MH, Gertz M. Venetoclax for the treatment of multiple myeloma. Expert Review of Hematology. 2018; 11: 915–920. https://doi.org/10.1080/17474086.2018.1548931

[22] Schwickart M, Huang X, Lill JR, Liu J, Ferrando R, French DM, et al. Deubiquitinase USP9X stabilizes MCL1 and promotes tumour cell survival. Nature. 2010; 463: 103–107. https://doi.org/10.1038/nature08646

[23] Ye G, Jiao Y, Deng L, Cheng M, Wang S, Zhang J, et al. Beauvericin suppresses the proliferation and pulmonary metastasis of osteosarcoma by selectively inhibiting TGFBR2 pathway. International Journal of Biological Sciences. 2023; 19: 4376–4392. https://doi.org/10.7150/ijbs.86214

[24] Jeong DH, Jung DW, Kim JW, Lee HS. Beauvericin, produced by Fusarium oxysporum inhibits bisphenol A-induced proliferation of human breast cancer cell line by regulating ERα/p38 pathway. The Journal of Steroid Biochemistry and Molecular Biology. 2024; 239: 106483. https://doi.org/10.1016/j.jsbmb.2024.106483

[25] Juan-García A, Ilie AM, Juan C, Martínez L. Evaluating the combined and individual cytotoxic effect of beauvericin, enniatin B and ochratoxin a on breast cancer cells, leukemia cells, and fresh peripheral blood mononuclear cells. Toxicology in Vitro. 2024; 99: 105890. https://doi.org/10.1016/j.tiv.2024.105890

[26] Carneiro BA, El-Deiry WS. Targeting apoptosis in cancer therapy. Nature Reviews. Clinical Oncology. 2020; 17: 395–417. https://doi.org/10.1038/s41571-020-0341-y

[27] Fonseca R, Zhu YX, Bruins LA, Ahmann J, de Bonolo Campos C, Braggio E, et al. Exploring BCL2 regulation and upstream signaling transduction in venetoclax resistance in multiple myeloma: potential avenues for therapeutic intervention. Blood Cancer Journal. 2025; 15: 10. https://doi.org/10.1038/s41408-025-01215-x

[28] Silbermann R, Roodman GD. Myeloma bone disease: Pathophysiology and management. Journal of Bone Oncology. 2013; 2: 59–69. https://doi.org/10.1016/j.jbo.2013.04.001

[29] Mitsiades N, Mitsiades CS, Poulaki V, Anderson KC, Treon SP. Intracellular regulation of tumor necrosis factor-related apoptosis-inducing ligand-induced apoptosis in human multiple myeloma cells. Blood. 2002; 99: 2162–2171. https://doi.org/10.1182/blood.v99.6.2162

[30] Lee C, Oh JI, Park J, Choi JH, Bae EK, Lee HJ, et al. TNF α mediated IL-6 secretion is regulated by JAK/STAT pathway but not by MEK phosphorylation and AKT phosphorylation in U266 multiple myeloma cells. BioMed Research International. 2013; 2013: 580135. https://doi.org/10.1155/2013/580135